



Growth and characterization of a new inorganic metal–halide crystal structure, InPb_2Cl_5

Michael P. Lewis, Ramjee Kandel, Gabriele Schatte and Peng L. Wang*

Department of Chemistry, Queen's University, Kingston, Ontario K7L 3N6, Canada. *Correspondence e-mail: wang.peng@chem.queensu.ca

Received 11 July 2023

Accepted 8 September 2023

Edited by S. Parkin, University of Kentucky, USA

Keywords: crystal structure; inorganic; InPb_2Cl_5 ; solid-state.

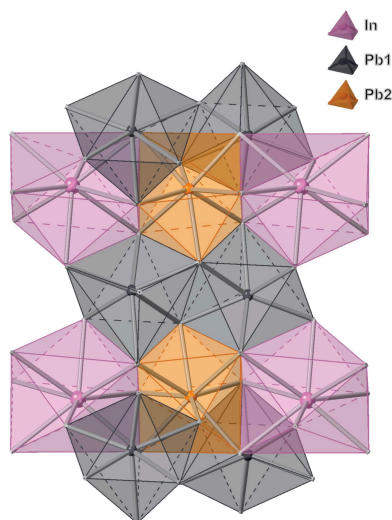
CCDC reference: 2294068

Supporting information: this article has supporting information at journals.iucr.org/e

A new solid-state inorganic compound, indium dilead pentachloride, InPb_2Cl_5 , was synthesized by melting InCl and PbCl_2 in a vacuum-sealed quartz ampoule. The ampoule was heated to 793 K and then slowly cooled to room temperature to induce crystallization of InPb_2Cl_5 . InPb_2Cl_5 crystallizes in the monoclinic crystal system adopting a space group of type $P2_1/c$, which is isostructural with other metal halides such as RbPb_2Cl_5 , KPb_2Cl_5 and TlPb_2Cl_5 . The bulk InPb_2Cl_5 exhibits a metallic black/grey colour, allowing it to be separated from white/yellow PbCl_2 crystals. Due to the incongruent nature of the compound, the pure bulk InPb_2Cl_5 was not obtained. The black/grey InPb_2Cl_5 crystals were characterized by powder and single-crystal X-ray diffraction. InPbCl_3 was also explored, however the growth was unsuccessful.

1. Chemical context

Indium lead chloride, InPb_2Cl_5 is a metal halide that has been studied as a new material to be used in optoelectronic semiconducting applications. Other isostructural metal halides that have the structure APb_2Cl_5 (where $A = \text{K}, \text{Rb}, \text{Tl}$) have gained interest in fields such as optoelectronics (Vu *et al.*, 2020), and photovoltaics as a tunable laser (Isaenko *et al.*, 2013; Khyzhun *et al.*, 2014; Brown *et al.*, 2013). There has been success in growing metal-halide semiconducting crystals such as RbPb_2Cl_5 and KPb_2Cl_5 (Isaenko *et al.*, 2013; Rowe *et al.*, 2014; Isaenko *et al.*, 2009), however single-crystal InPb_2Cl_5 has not been reported and has only been computationally studied as the InPbCl_3 phase (Khan *et al.*, 2022). Similar to RbPb_2Cl_5 , KPb_2Cl_5 , and TlPb_2Cl_5 , InPb_2Cl_5 crystallizes in a monoclinic structure and has a space group of type $P2_1/c$. Bulk InPb_2Cl_5 samples were prepared, which contained a mixture of black/grey metallic polycrystalline InPb_2Cl_5 at the bottom of the ampoule and white/yellow PbCl_2 crystals above. When the black/grey crystals were broken up, the crystals appeared to have a much clearer and lighter green hue. The broken-up crystal was examined under an optical microscope and clear colourless crystal pieces were seen. The clear colourless single-crystal pieces were handpicked and characterized by single-crystal X-ray diffraction (XRD). The bulk material was ground using a mortar and pestle and the powder was characterized by powder-XRD. The powder-XRD pattern had low intensity peaks of In_7Cl_9 and PbCl_2 impurities, but matched closely with the InPb_2Cl_5 phase. When InPb_2Cl_5 was left in ambient conditions over four months, the bulk absorbed moisture over time and left a light-grey film around the bulk with moisture build up on the side of the material.



OPEN ACCESS

Published under a CC BY 4.0 licence

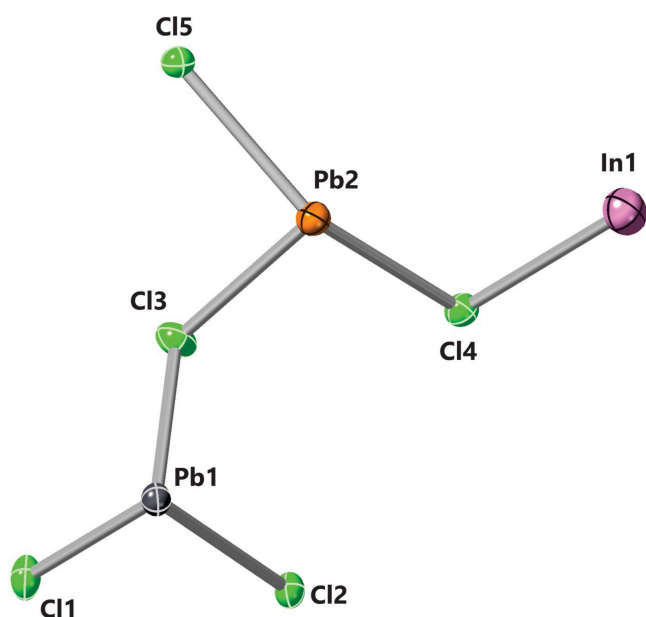
Table 1

 Bond lengths (Å) in the InPb_2Cl_5 asymmetric unit (Fig. 1).

Bond	Distance
Cl1—Pb1	2.8677 (12)
Cl2—Pb1	2.9214 (10)
Cl3—Pb1	2.8744 (12)
Cl3—Pb2	2.9156 (12)
Cl4—Pb2	2.9236 (11)
Cl5—Pb2	2.9760 (12)

2. Structural commentary

The single-crystal structure of InPb_2Cl_5 was found to adopt a monoclinic $P2_1/c$ space group. The single-crystal structure refinement confirmed the composition as InPb_2Cl_5 . The bond lengths in the asymmetric unit (Fig. 1) of InPb_2Cl_5 are listed in Table 1. The unit cell of InPb_2Cl_5 (Fig. 2) has four symmetry-related formula units. The Pb atoms in the unit cell (Fig. 2) coordinate multiple chlorine atoms that give a range of bond lengths from 2.868 (5)–3.3145 (15) Å. The Pb1 atoms coordinate with seven chlorine atoms in the structure, with bond lengths ranging from 2.868 (5)–3.1371 (14) Å. The Pb1 atoms form a nine-face polyhedron with a volume of 37.374 Å³ (Fig. 3). The Pb2 atoms have a coordination number of 8 with bond lengths from 2.916 (7)–3.3145 (15) Å. The Pb2 atoms form a 12-face dodecahedron with a volume of 49.796 Å³ (Fig. 3). The shortest bond length is between Cl1 and Pb1, which is 2.868 (5) Å. The largest bond lengths are between the Pb2 atom and a Cl3 atom at 3.3145 (15) Å. The typical bond length between Pb and Cl atoms is 2.44 Å in the binary structure. There is an increase in bond lengths from the binary PbCl_2 to the InPb_2Cl_5 structure. The indium atom interstitially coordinates eight chlorine atoms in a distorted octahedral geometry. The range of indium–chlorine bonds range from


Figure 1

A view of the asymmetric unit. Ellipsoids are drawn at the 50% probability level.

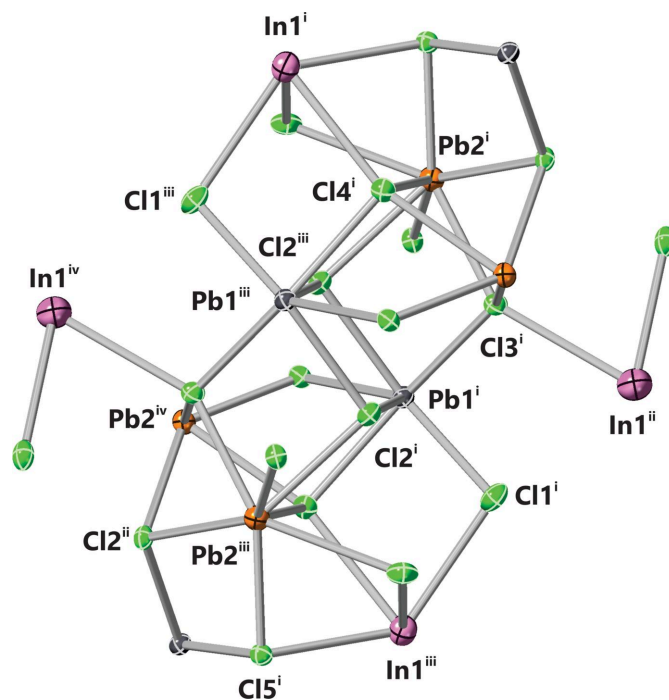
Table 2
 InPb_2Cl_5 unit-cell parameters compared with isostructural compounds.

Compound	<i>a</i> (Å)	<i>b</i> (Å)	<i>c</i> (Å)	β (°)	Volume (Å ³)
InPb_2Cl_5	8.9681 (11)	7.9033 (9)	12.4980 (16)	90.254 (6)	885.82 (19)
TlPb_2Cl_5	8.9561	7.9204	12.4908	90.073	886.0
RbPb_2Cl_5	8.9900	7.9963	12.541	90.20	901.5
KPb_2Cl_5	8.864	7.932	12.491	90.153	878.2

3.1447 (18)–3.588 (8) Å. The indium atom forms a 12-face dodecahedron with a volume of 62.568 Å³ (Fig. 3). The typical In–Cl bond length is around 2.56 Å, indicating that the indium–chlorine bonds have a much weaker interaction in the InPb_2Cl_5 structure. The largest bond angles seen in the unit cell (Fig. 2) are between the Cl1ⁱⁱⁱ–Pb1–Cl2 atoms at 156.02 (3)° (symmetry codes as per Fig. 2). The shortest bond angle in the structure is between the Cl4ⁱⁱ–In1–Cl5ⁱ atoms at 63.2587 (3)°. The Pb atoms have stronger interactions with the chlorine atoms resulting in shorter bond lengths and a wide range of bond lengths from 69.7087 (3)–156.02 (3)°. The indium atoms have weaker interactions and are interstitially located throughout the structure. The weaker interactions of the indium atoms is evident because of the shorter bond lengths and smaller range of bond angles from 63.2587 (3)–144.1653 (3)°. A complete list of bond lengths and bond angles is given in the supporting information.

3. Database survey

The InPb_2Cl_5 structure is isostructural with other compounds such as RbPb_2Cl_5 (Isaenko *et al.*, 2013; Isaenko *et al.*, 2009),


Figure 2

A partial packing plot viewed down the *b*-axis. Ellipsoids are drawn at the 50% probability level. Symmetry codes: (i) *x*, *y*, *z*; (ii) $-x$, $y + \frac{1}{2}$, $-z + \frac{1}{2}$; (iii) $-x$, $-y$, $-z$; (iv) x , $-y - \frac{1}{2}$, $z - \frac{1}{2}$.

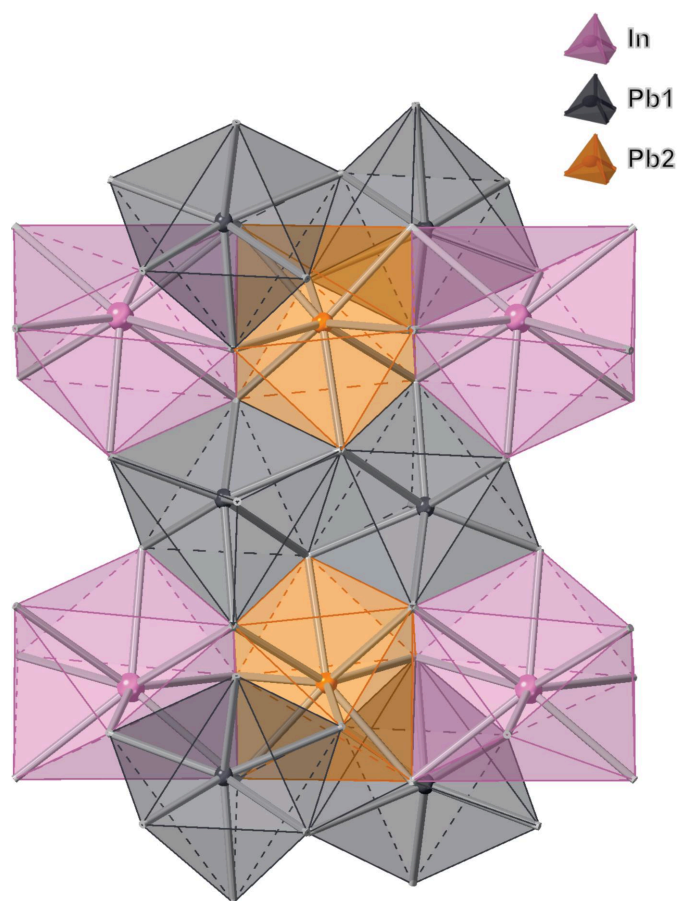


Figure 3
A polyhedron view of the crystal structure packing, viewed down the *b*-axis.

KPb_2Cl_5 (Rowe *et al.*, 2014; Isaenko *et al.*, 2009) and TlPb_2Cl_5 (Khyzhun *et al.*, 2014). The cell dimensions of the monoclinic InPb_2Cl_5 cell are compared with the isostructural compounds in Table 2. The cell dimensions for InPb_2Cl_5 match very closely with TlPb_2Cl_5 . There is no significant difference between the InPb_2Cl_5 structure and the isostructural structures in Table 2, the small difference is due to the atomic size difference for indium. The indium atom has the smallest atom size, so it is expected to fit tighter into the unit cell compared to the other structures, so we see that InPb_2Cl_5 has the smallest unit cell volume. The thallium atom is most comparable to the indium atom size, which is why its cell dimensions are most similar.

4. Synthesis and crystallization

Stoichiometric amounts of the binary compounds $\text{In}^{\text{I}}\text{Cl}$ (4g, ThermoFisher Scientific 99.995%, metals basis) and $\text{Pb}^{\text{II}}\text{Cl}_2$ [3.7278 (5)g, Acros Organics 99%] were mixed in a glove box under an argon environment ($<0.1\text{ppm O}_2$ and H_2O). The binary compounds were ground together with a mortar and pestle and then loaded into a quartz ampoule. The quartz ampoule was flame sealed under high vacuum (5.5×10^{-5} mbar). The loaded quartz ampoule was heated at 3K min^{-1} in a vertical furnace to 793K. The ampoule was cooled at

Table 3
Experimental details.

Crystal data	$\text{In}_2\text{Pb}_4\text{Cl}_{10}$
Chemical formula	1412.9
M_r	Monoclinic, $P2_1/c$
Crystal system, space group	298
Temperature (K)	8.9681 (11), 7.9033 (9), 12.4980 (16)
a, b, c (Å)	90.254 (6)
β (°)	885.82 (19)
V (Å ³)	2
Z	Mo $K\alpha$
Radiation type	41.91
μ (mm ⁻¹)	$0.22 \times 0.18 \times 0.13$
Crystal size (mm)	
Data collection	
Diffractometer	Bruker APEXII CCD
Absorption correction	Multi-scan (<i>SADABS</i> ; Krause <i>et al.</i> , 2015)
$T_{\text{min}}, T_{\text{max}}$	0.378, 0.746
No. of measured, independent and observed [$I > 2\sigma(I)$] reflections	20682, 2699, 2423
R_{int}	0.051
$(\sin \theta/\lambda)_{\text{max}}$ (Å ⁻¹)	0.715
Refinement	
$R[F^2 > 2\sigma(F^2)], wR(F^2), S$	0.021, 0.042, 1.08
No. of reflections	2699
No. of parameters	74
$\Delta\rho_{\text{max}}, \Delta\rho_{\text{min}}$ (e Å ⁻³)	1.22, -1.13

Computer programs: *APEX2* and *SAINT* (Bruker, 2012), *SHELXT* (Sheldrick, 2015a), *SHELXL* (Sheldrick, 2015b), *CrystalMaker* (Palmer, 2014), *WinGX* (Farrugia, 2012) and *publCIF* (Westrip, 2010).

0.5 K min^{-1} to room temperature. A 1 mm^3 piece of the metallic black and grey crystal was separated from the excess yellow $\text{Pb}^{\text{II}}\text{Cl}_2$ crystals and sent for characterization by powder-XRD and single-crystal XRD.

5. Refinement

The crystallographic data, data collection and structure refinement are summarized in Table 3.

Acknowledgements

The authors would like to thank Queen's University and the Arthur B. Macdonald Institute for funding.

Funding information

Funding for this research was provided by: Natural Sciences and Engineering Research Council of Canada; Canada Foundation for Innovation; Canada First Research Excellence Fund.

References

- Brown, E., Hanley, C. B., Hömmerich, U., Bluiett, A. G. & Trivedi, S. B. (2013). *J. Lumin.* **133**, 244–248.
 Bruker (2012). *APEX2* and *SAINT*. Bruker AXS Inc, Madison, Wisconsin, USA.
 Farrugia, L. J. (2012). *J. Appl. Cryst.* **45**, 849–854.

- Isaenko, L. I., Merkulov, A. A., Tarasova, A. Yu., Pashkov, V. M. & Drebuschak, V. A. (2009). *J. Therm. Anal. Calorim.* **95**, 323–325.
- Isaenko, L. I., Ogorodnikov, I. N., Pustovarov, V. A., Tarasova, A. Yu. & Pashkov, V. M. (2013). *Opt. Mater.* **35**, 620–625.
- Khan, S., Mehmood, N., Ahmad, R., Kalsoom, A. & Hameed, K. (2022). *Mater. Sci. Semicond. Process.* **150**, 106973.
- Khyzhun, O. Y., Bekenev, V. L., Denysyuk, N. M., Parasyuk, O. V. & Fedorchuk, A. O. (2014). *J. Alloys Compd.* **582**, 802–809.
- Krause, L., Herbst-Irmer, R., Sheldrick, G. M. & Stalke, D. (2015). *J. Appl. Cryst.* **48**, 3–10.
- Palmer, D. C. (2014). *CrystalMaker*. CrystalMaker Software Ltd, Begbroke, Oxfordshire, England.
- Rowe, E., Tupitsyn, E., Bhattacharya, P., Matei, L., Groza, M., Buliga, V., Atkinson, G. & Burger, A. (2014). *J. Cryst. Growth*, **393**, 156–158.
- Sheldrick, G. M. (2015a). *Acta Cryst.* **A71**, 3–8.
- Sheldrick, G. M. (2015b). *Acta Cryst.* **C71**, 3–8.
- Vu, T. V., Lavrentyev, A. A., Gabrelian, B. V., Vo, D. D., Pham, K. D., Denysyuk, N. M., Isaenko, L. I., Tarasova, A. Y. & Khyzhun, O. Y. (2020). *Opt. Mater.* **102**, 109793.
- Westrip, S. P. (2010). *J. Appl. Cryst.* **43**, 920–925.

supporting information

Acta Cryst. (2023). E79, 942-945 [https://doi.org/10.1107/S2056989023007892]

Growth and characterization of a new inorganic metal–halide crystal structure, InPb_2Cl_5

Michael P. Lewis, Ramjee Kandel, Gabriele Schatte and Peng L. Wang

Computing details

Cell refinement: *APEX2* (Bruker, 2012); data reduction: *S SAINT* (Bruker, 2012); program(s) used to solve structure: *SHELXT* (Sheldrick, 2015a); program(s) used to refine structure: *SHELXL* (Sheldrick, 2015b); molecular graphics: *CrystalMaker* (Palmer, 2014); software used to prepare material for publication: *WinGX* (Farrugia, 2012) and *publCIF* (Westrip, 2010).

Indium dilead pentachloride

Crystal data

$\text{In}_2\text{Pb}_4\text{Cl}_{10}$	$F(000) = 1192$
$M_r = 1412.9$	$D_x = 5.297 \text{ Mg m}^{-3}$
Monoclinic, $P2_1/c$	Mo $K\alpha$ radiation, $\lambda = 0.71073 \text{ \AA}$
Hall symbol: $-P 2_1/c$	Cell parameters from 9997 reflections
$a = 8.9681 (11) \text{ \AA}$	$\theta = 2.3\text{--}30.5^\circ$
$b = 7.9033 (9) \text{ \AA}$	$\mu = 41.91 \text{ mm}^{-1}$
$c = 12.4980 (16) \text{ \AA}$	$T = 298 \text{ K}$
$\beta = 90.254 (6)^\circ$	Transparent square, colourless
$V = 885.82 (19) \text{ \AA}^3$	$0.22 \times 0.18 \times 0.13 \text{ mm}$
$Z = 2$	

Data collection

Bruker APEXII CCD diffractometer	$T_{\min} = 0.378, T_{\max} = 0.746$
Radiation source: sealed X-ray tube, Incoatec $\text{I}\mu\text{s}$	20682 measured reflections
Graphite monochromator	2699 independent reflections
Detector resolution: $7.9 \text{ pixels mm}^{-1}$	2423 reflections with $I > 2\sigma(I)$
φ and ω scans	$R_{\text{int}} = 0.051$
Absorption correction: multi-scan (SADABS; Krause <i>et al.</i> , 2015)	$\theta_{\max} = 30.6^\circ, \theta_{\min} = 2.3^\circ$
	$h = -12 \rightarrow 12$
	$k = -11 \rightarrow 11$
	$l = -17 \rightarrow 17$

Refinement

Refinement on F^2	Primary atom site location: structure-invariant direct methods
Least-squares matrix: full	$w = 1/[\sigma^2(F_o^2) + (0.0083P)^2 + 1.8133P]$
$R[F^2 > 2\sigma(F^2)] = 0.021$	where $P = (F_o^2 + 2F_c^2)/3$
$wR(F^2) = 0.042$	$(\Delta/\sigma)_{\max} = 0.002$
$S = 1.08$	$\Delta\rho_{\max} = 1.22 \text{ e \AA}^{-3}$
2699 reflections	$\Delta\rho_{\min} = -1.13 \text{ e \AA}^{-3}$
74 parameters	
0 restraints	
0 constraints	

Extinction correction: SHELXL-2018/3
(Sheldrick 2015b),
 $F_c^* = kFc[1 + 0.001xFc^2\lambda^3/\sin(2\theta)]^{-1/4}$
Extinction coefficient: 0.00232 (8)

Special details

Geometry. All esds (except the esd in the dihedral angle between two l.s. planes) are estimated using the full covariance matrix. The cell esds are taken into account individually in the estimation of esds in distances, angles and torsion angles; correlations between esds in cell parameters are only used when they are defined by crystal symmetry. An approximate (isotropic) treatment of cell esds is used for estimating esds involving l.s. planes.

Fractional atomic coordinates and isotropic or equivalent isotropic displacement parameters (\AA^2)

	<i>x</i>	<i>y</i>	<i>z</i>	$U_{\text{iso}}^*/U_{\text{eq}}$
Cl1	0.04109 (12)	0.67574 (15)	0.41739 (11)	0.0316 (3)
Cl2	0.45758 (11)	0.66555 (13)	0.40434 (9)	0.0226 (2)
Cl3	0.27835 (14)	0.65746 (14)	0.68735 (10)	0.0304 (3)
Cl4	0.72918 (12)	0.68702 (14)	0.72264 (9)	0.0252 (2)
Cl5	0.28105 (12)	0.45943 (14)	1.00167 (9)	0.0232 (2)
In1	0.98678 (5)	0.45346 (6)	0.83468 (4)	0.04410 (11)
Pb1	0.24664 (2)	0.43551 (2)	0.50647 (2)	0.02229 (6)
Pb2	0.49498 (2)	0.48805 (2)	0.82509 (2)	0.02538 (6)

Atomic displacement parameters (\AA^2)

	U^{11}	U^{22}	U^{33}	U^{12}	U^{13}	U^{23}
Cl1	0.0194 (5)	0.0309 (6)	0.0445 (7)	0.0009 (4)	0.0017 (5)	0.0137 (5)
Cl2	0.0192 (5)	0.0201 (4)	0.0285 (6)	−0.0008 (4)	−0.0002 (4)	0.0059 (4)
Cl3	0.0364 (6)	0.0283 (5)	0.0263 (6)	0.0084 (5)	−0.0081 (5)	−0.0063 (4)
Cl4	0.0259 (5)	0.0254 (5)	0.0243 (6)	−0.0027 (4)	0.0021 (4)	0.0025 (4)
Cl5	0.0251 (5)	0.0240 (5)	0.0205 (5)	0.0004 (4)	0.0005 (4)	0.0009 (4)
In1	0.0418 (2)	0.0432 (2)	0.0472 (3)	0.00874 (18)	−0.00359 (19)	−0.00495 (19)
Pb1	0.01876 (9)	0.02412 (9)	0.02399 (10)	−0.00042 (6)	−0.00025 (6)	−0.00142 (6)
Pb2	0.02614 (10)	0.02526 (9)	0.02473 (10)	−0.00304 (7)	0.00037 (7)	0.00179 (6)

Geometric parameters (\AA , $^\circ$)

Cl1—Pb1	2.8677 (12)	Cl3—Pb2	2.9156 (12)
Cl1—Pb1 ⁱ	2.8912 (11)	Cl4—Pb2	2.9236 (11)
Cl2—Pb1	2.9214 (10)	Cl4—Pb1 ⁱⁱⁱ	3.0314 (12)
Cl2—Pb2 ⁱⁱ	2.9311 (10)	Cl5—Pb2	2.9394 (11)
Cl2—Pb1 ⁱⁱⁱ	2.9817 (11)	Cl5—Pb2 ^{iv}	2.9760 (12)
Cl3—Pb1	2.8744 (12)		
Pb1—Cl1—Pb1 ⁱ	104.12 (4)	Cl2—Pb1—Cl2 ⁱⁱⁱ	75.72 (3)
Pb1—Cl2—Pb2 ⁱⁱ	143.53 (4)	Cl1—Pb1—Cl4 ⁱⁱⁱ	83.88 (4)
Pb1—Cl2—Pb1 ⁱⁱⁱ	104.28 (3)	Cl3—Pb1—Cl4 ⁱⁱⁱ	158.52 (3)
Pb2 ⁱⁱ —Cl2—Pb1 ⁱⁱⁱ	105.88 (3)	Cl1 ⁱ —Pb1—Cl4 ⁱⁱⁱ	106.34 (4)
Pb1—Cl3—Pb2	104.33 (4)	Cl2—Pb1—Cl4 ⁱⁱⁱ	74.75 (3)

Pb2—C14—Pb1 ⁱⁱⁱ	107.24 (4)	C12 ⁱⁱⁱ —Pb1—C14 ⁱⁱⁱ	101.55 (3)
Pb2—C15—Pb2 ^{iv}	95.44 (3)	C13—Pb2—C14	88.42 (4)
C11—Pb1—C13	87.85 (4)	C13—Pb2—C12 ^v	72.16 (3)
C11—Pb1—C11 ⁱ	75.88 (4)	C14—Pb2—C12 ^v	74.28 (3)
C13—Pb1—C11 ⁱ	90.69 (4)	C13—Pb2—C15	92.48 (3)
C11—Pb1—C12	80.49 (3)	C14—Pb2—C15	147.44 (3)
C13—Pb1—C12	84.37 (4)	C12 ^v —Pb2—C15	75.06 (3)
C11 ⁱ —Pb1—C12	156.02 (3)	C13—Pb2—C15 ^{iv}	144.23 (3)
C11—Pb1—C12 ⁱⁱⁱ	153.09 (3)	C14—Pb2—C15 ^{iv}	76.10 (3)
C13—Pb1—C12 ⁱⁱⁱ	77.57 (3)	C12 ^v —Pb2—C15 ^{iv}	72.65 (3)
C11 ⁱ —Pb1—C12 ⁱⁱⁱ	126.11 (3)	C15—Pb2—C15 ^{iv}	84.56 (3)

Symmetry codes: (i) $-x, -y+1, -z+1$; (ii) $x, -y+3/2, z-1/2$; (iii) $-x+1, -y+1, -z+1$; (iv) $-x+1, -y+1, -z+2$; (v) $x, -y+3/2, z+1/2$.